

Dynamical entanglement of vibrations in small molecules through an analytically algebraic approach

Yan Liu,^{1,2} Yujun Zheng,^{1,*} Weiyi Ren,² and Shiliang Ding¹¹*School of Physics, Shandong University, Jinan 250100, China*²*School of Physics and Electronic Information, China West Normal University, Nanchong 637002, China*

(Received 5 November 2007; revised manuscript received 16 January 2008; published 30 September 2008)

We study the dynamical entanglement of vibrations in small molecules by employing algebraic models. We analytically obtain the linear entropy, von Neumann entropy, and the Lyapunov function for the integrable dimer and realistic small molecules for both initial Fock states and coherent states. The contributions of states to the dynamical entropy are also investigated.

DOI: [10.1103/PhysRevA.78.032523](https://doi.org/10.1103/PhysRevA.78.032523)

PACS number(s): 33.15.-e, 33.20.Tp, 03.67.Mn

I. INTRODUCTION

Entanglement, one of the most interesting features of quantum mechanics and a potentially useful resource of quantum states exhibiting correlations, has stimulated theoretical studies of various quantum systems [1–6]. Most of those studies are devoted to characterizing dynamical properties of entanglement of the ground state or pure states in ideal theoretical models. The continuous-variable-type entangled states including squeezed states and coherent states have also been studied [7,8].

Entanglement has various interesting properties [2,8,9], for example, a sharp singularity at or near the phase transition point and scaling behavior. Several measures of quantum entanglement have been introduced, such as entanglement of formation, entanglement of distillation, relative entropy, linear entropy, von Neumann entropy, Renyi entropy, negativity, and concurrence, etc. [2,4,8–13]. The most natural measurement of the uncertainty of the quantum mechanical state is arguably the entropy. Physically, entropy can be interpreted as a measurement of the disorder of the system. Both the linear entropy and von Neumann entropy are commonly used to measure deviations from pure state behavior, such as in the process of decoherence [14–17]. The general properties of the two entropies are similar, and their values of zero could be used to predict the purification time. The linear entropy can also be used to describe the degree of purity of the subsystem in a scale from 0 (pure state) to 1 (statistical mixture).

The interesting phenomena exhibited by the closed two-site systems (dimer) have been studied [18–22]. Based on the molecular vibrations of small molecules, the physical implementation of quantum computation was studied [23–25]. Yet there appear to be few investigations of dynamical entanglement for realistic molecular systems and the two-site dimer system.

In this work we analytically investigate the linear entropy, the von Neumann entropy, and the Lyapunov function for initial Fock states and coherent states for *the integrable dimer* and *realistic small molecules* systems. The realistic small algebraic molecular Hamiltonian suggested by Kell-

man [26] was employed in our investigation. This Hamiltonian has been successfully used to study many aspects of small molecules [7,27–30].

This paper is structured as follows. In Sec. II, analytical expressions for the linear and von Neumann entropy for both initial Fock and coherent states are derived. The Lyapunov functions of the integrable dimer and the realistic small symmetric molecules are also calculated for initial Fock states. In Sec. III, for initial Fock states, we discuss the entanglement, the probabilities of states, and the relation between entanglement and the phase transition point for the integrable dimer and small symmetric molecules. We also investigate the entanglement dynamics of the two models for initial coherent states in this section. The paper ends with some concluding remarks in Sec. IV.

II. THEORETICAL FRAMEWORK

A. General considerations

For a given quantum system with time-independent Hamiltonian \mathcal{H} , the evolution can be obtained by

$$|\psi(t)\rangle = e^{-i\mathcal{H}t}|\psi(0)\rangle, \quad (1)$$

where $|\psi(0)\rangle$ is the initial state of the system. Here we assume $\hbar=1$. We can extract all the dynamical information of the quantum system from the time-dependent wave function $|\psi(t)\rangle$. In this work we are interested in the dynamical entanglement of two types of quantum system: the integrable dimer and realistic small molecules.

The algebraic Hamiltonian of the integrable dimer is given by [22]

$$\begin{aligned} \mathcal{H} = & \frac{5}{4} + \frac{3}{2}(a_1^\dagger a_1 + a_2^\dagger a_2) + \frac{1}{2}[(a_1^\dagger a_1)^2 + (a_2^\dagger a_2)^2] \\ & + c(a_1^\dagger a_2 + a_2^\dagger a_1) \equiv \mathcal{H}_0 + \mathcal{H}_1, \end{aligned} \quad (2)$$

where a_i and a_i^\dagger ($i=1,2$) are the annihilation and creation operators on site i . The classical and quantum properties for this system were studied in Ref. [22]. In Eq. (2), we let

$$\mathcal{H}_0 = \frac{5}{4} + \frac{3}{2}(a_1^\dagger a_1 + a_2^\dagger a_2) + \frac{1}{2}[(a_1^\dagger a_1)^2 + (a_2^\dagger a_2)^2 + 2a_1^\dagger a_1 a_2^\dagger a_2],$$

*yzheng@sdu.edu.cn

$$\mathcal{H}_1 = -a_1^\dagger a_1 a_2^\dagger a_2 + c(a_1^\dagger a_2 + a_2^\dagger a_1). \quad (3)$$

It is easy to check that Hamiltonians \mathcal{H}_0 and \mathcal{H}_1 satisfy the following commutation relation:

$$[\mathcal{H}_0, \mathcal{H}_1] = 0. \quad (4)$$

This quantum Hamiltonian, Eq. (2), conserves the total boson number $N = n_1 + n_2$, where $n_i = a_i^\dagger a_i$ ($i=1,2$) is the boson number on site i . The number N in this integrable dimer Hamiltonian can correspond physically to the total particle number of the two interacting BECs or the total number of photons associated with the field modes interacting in a Kerr medium [31,32]. This Hamiltonian (2) can be used to calculate the vibrational spectra of polyatomic molecules [33].

The algebraic Hamiltonian of a realistic symmetric small molecule can be written as [26,30]

$$\begin{aligned} \mathcal{H} = & \omega_0(n_1 + n_2 + 1) + \frac{\alpha}{2} \left[\left(n_1 + \frac{1}{2} \right)^2 + \left(n_2 + \frac{1}{2} \right)^2 \right] \\ & + \alpha_{12} \left(n_1 + \frac{1}{2} \right) \left(n_2 + \frac{1}{2} \right) + \frac{1}{2} \left[\beta + \frac{\varepsilon}{2} (n_1 + n_2 + 1) \right] \\ & \times (a_1^\dagger a_2 + a_2^\dagger a_1) + \delta' (a_1^\dagger a_1^\dagger a_2 a_2 + a_2^\dagger a_2^\dagger a_1 a_1) \equiv \mathcal{H}_0 + \mathcal{H}_1, \end{aligned} \quad (5)$$

where a_i and a_i^\dagger ($i=1,2$) are the annihilation and creation operators on local mode i . In Eq. (5), we defined

$$\mathcal{H}_0 = \omega_0(n_1 + n_2 + 1) \quad \text{and} \quad \mathcal{H}_1 = \mathcal{H} - \mathcal{H}_0. \quad (6)$$

The symmetric molecular Hamiltonian conserves the multiplet quantum numbers $N = n_1 + n_2$; $n_i = a_i^\dagger a_i$ is the vibrational quantum number on local mode i ($i=1,2$). It is obvious that the \mathcal{H}_0 and \mathcal{H}_1 in Eq. (5) also satisfy Eq. (4).

Since we are interested in dynamical entanglement, the total density operator is a projector onto the state $|\psi(t)\rangle$,

$$\rho(t) = |\psi(t)\rangle\langle\psi(t)|, \quad (7)$$

and the reduced density matrices

$$\rho_1(t) = \text{Tr}_2 \rho(t) = \text{Tr}_2 |\psi(t)\rangle\langle\psi(t)|, \quad (8)$$

where Tr_2 is the partial trace over subsystem 2.

The entanglement can be described by linear entropy $S_l(t)$ and von Neumann entropy $S_n(t)$, which are defined by [34,35]

$$S_l(t) = 1 - \text{Tr}_1 \rho_1(t)^2,$$

$$S_n(t) = -\text{Tr}_1 [\rho_1(t) \ln \rho_1(t)]. \quad (9)$$

Some studies of stability and other characteristics of dynamical systems employ the direct Lyapunov method. The Lyapunov function has been used to study the stability of the quantum control system [36–38]. Here we employ the

Lyapunov function $\mathcal{V}(t)$ to describe the “distance” between the final state $|\psi(t)\rangle$ and the initial state $|\psi(0)\rangle$ at time t [36–39],

$$\mathcal{V}(t) = 1 - |\langle\psi(0)|\psi(t)\rangle|^2. \quad (10)$$

We can see its zero values describe the recurrence times from the definition.

In the following subsections we will consider two useful initial states: *Fock states* and *coherent states* for the two algebraic models: integrable dimer and *small symmetric molecules*.

B. Fock states

We first consider the case of initially unitary separable Fock states,

$$|\psi(0)\rangle = |n_0\rangle \otimes |N - n_0\rangle \equiv |n_0, N - n_0\rangle, \quad (11)$$

where n_0 can be an arbitrary integer between 0 and N . The time evolution of the system, from Eq. (1), is given by

$$\begin{aligned} |\psi(t)\rangle &= e^{-it\mathcal{H}} |\psi(0)\rangle = e^{-it\mathcal{H}_0} e^{-it\mathcal{H}_1} |n_0, N - n_0\rangle \\ &\equiv \mathcal{U}_0(t) \mathcal{U}_1(t) |n_0, N - n_0\rangle, \end{aligned} \quad (12)$$

since $\mathcal{H} = \mathcal{H}_0 + \mathcal{H}_1$, and \mathcal{H}_0 and \mathcal{H}_1 satisfy Eq. (4).

1. Integrable dimer

For the integrable dimer system, after we consider the basic relation

$$\begin{aligned} a^\dagger |n\rangle &= \sqrt{n+1} |n+1\rangle, \\ a |n\rangle &= \sqrt{n} |n-1\rangle, \end{aligned} \quad (13)$$

and the Hamiltonian \mathcal{H}_1 act on the Fock states $|n_1, n_2\rangle$,

$$\begin{aligned} \mathcal{H}_1 |n_1, n_2\rangle &= -n_1 n_2 |n_1, n_2\rangle + c \sqrt{(n_1+1)n_2} |n_1+1, n_2-1\rangle \\ &\quad + c \sqrt{n_1(n_2+1)} |n_1-1, n_2+1\rangle, \end{aligned} \quad (14)$$

we have, after some algebra,

$$\begin{aligned} \mathcal{U}_1(t) &\equiv e^{-it\mathcal{H}_1} |n_0, N - n_0\rangle \\ &= \sum_{k=0}^{\infty} \frac{(-it)^k}{k!} \mathcal{H}_1^k |n_0, N - n_0\rangle \\ &= \sum_{k=0}^{\infty} \sum_{l=\zeta}^{\xi} C_k^{(l)}(t) |n_0 + l, N - n_0 - l\rangle \\ &= \sum_{l=-n_0}^{N-n_0} P^{(l)}(t) |n_0 + l, N - n_0 - l\rangle, \end{aligned} \quad (15)$$

where $\zeta = \max\{-k, -n_0\}$, $\xi = \min\{k, N - n_0\}$, and $P^{(l)}(t) = \sum_{k=|l|}^{\infty} C_k^{(l)}(t)$.

The recursion expression of $C_k^{(l)}(t)$ is given by

$$C_k^{(l)}(t) = -\frac{it}{k} \{ - (n_0 + l)(N - n_0 - l)C_{k-1}^{(l)}(t) + c\sqrt{(n_0 + l + 1)(N - n_0 - l)}C_{k-1}^{(l+1)}(t) + c\sqrt{(n_0 + l)(N - n_0 - l + 1)}C_{k-1}^{(l-1)}(t) \}, \quad (16)$$

where $k=0, 1, 2, \dots, \infty$, and $C_0^{(l)}(t) = \delta_{0,l}$ for $k=0$.

2. Small symmetric molecule

The algebraic Hamiltonian of small symmetric molecules, Eq. (5), has been successfully used to study the vibrational levels and other properties [26,30]. Following a similar procedure to that employed for the integrable dimer model, the evolution operator of molecular system can be written

$$\begin{aligned} \mathcal{U}_1(t) &\equiv e^{-it\mathcal{H}_1}|n_0, N - n_0\rangle \\ &= \sum_{k=0}^{\infty} \frac{(-it)^k}{k!} \mathcal{H}_1^k |n_0, N - n_0\rangle \\ &= \sum_{k=0}^{\infty} \sum_{l=\xi}^{\xi} C_k^{(l)}(t) |n_0 + l, N - n_0 - l\rangle \\ &= \sum_{l=-n_0}^{N-n_0} P^{(l)}(t) |n_0 + l, N - n_0 - l\rangle, \end{aligned} \quad (17)$$

where $\xi = \max\{-k, -n_0\}$, $\xi = \min\{k, N - n_0\}$, and $P^{(l)}(t) = \sum_{k=|l|}^{\infty} C_k^{(l)}(t)$.

Similarly, the recursion expression of $C_k^{(l)}(t)$ is given by

$$\begin{aligned} C_k^{(l)}(t) &= \frac{-it}{k} \left(\left\{ \frac{\alpha}{2} \left[\left(n_0 + l + \frac{1}{2} \right)^2 + \left(N - n_0 - l + \frac{1}{2} \right)^2 \right] + \alpha_{12} \left(n_0 + l + \frac{1}{2} \right) \left(N - n_0 - l + \frac{1}{2} \right) \right\} C_{k-1}^{(l)}(t) \right. \\ &\quad + c\sqrt{(n_0 + l + 1)(N - n_0 - l)}C_{k-1}^{(l+1)}(t) + c\sqrt{(n_0 + l)(N - n_0 - l + 1)}C_{k-1}^{(l-1)}(t) \\ &\quad + \delta' \sqrt{(n_0 + l + 2)(N - n_0 - l - 1)(n_0 + l + 1)(N - n_0 - l)}C_{k-1}^{(l+2)}(t) \\ &\quad \left. + \delta' \sqrt{(n_0 + l - 1)(N - n_0 - l + 2)(n_0 + l)(N - n_0 - l + 1)}C_{k-1}^{(l-2)}(t) \right), \end{aligned} \quad (18)$$

where $c = \frac{1}{2}[\beta + \frac{\epsilon}{2}(N + 1)]$, $k=0, 1, 2, \dots, \infty$ and $C_0^{(l)}(t) = \delta_{0,l}$ for $k=0$.

Equations (15) and (17) give similar expressions for the $\mathcal{U}_1(t)$ for the two quantum systems, and the time evolution state can be generally written as follows:

$$|\psi(t)\rangle = \mathcal{U}_0 \sum_{l=-n_0}^{N-n_0} P^{(l)}(t) |n_0 + l, N - n_0 - l\rangle, \quad (19)$$

where $\mathcal{U}_0 = \exp[-it(5/4 + \frac{3}{2}N + 1/2N^2)]$ for the integrable dimer system and $\mathcal{U}_0 = e^{-itw_0(N+1)}$ for the realistic small molecules. The evolution of the two systems are now in a similar form, which is convenient for us. Clearly, the term \mathcal{U}_0 has no contribution to the dynamical entanglement. The density matrices are then given by

$$\begin{aligned} \rho(t) = |\psi(t)\rangle\langle\psi(t)| &= \sum_{l=-n_0}^{N-n_0} \sum_{l'=-n_0}^{N-n_0} P^{(l)}(t)P^{(l')}(t)^* |n_0 + l, N - n_0 - l\rangle \\ &\quad \times \langle n_0 + l', N - n_0 - l'|. \end{aligned} \quad (20)$$

The reduced density matrix traced over subsystem 2 is given by

$$\begin{aligned} \rho_1(t) = \text{Tr}_2 \rho(t) &= \sum_{n_2} \langle n_2 | \rho(t) | n_2 \rangle \\ &= \sum_{l=-n_0}^{N-n_0} \sum_{l'=-n_0}^{N-n_0} P^{(l)}(t)P^{(l')}(t)^* |n_0 + l\rangle\langle n_0 + l'| \delta_{l,l'} \\ &= \sum_{l=-n_0}^{N-n_0} |P^{(l)}(t)|^2 |n_0 + l\rangle\langle n_0 + l|. \end{aligned} \quad (21)$$

The reduced density matrix $\rho_1(t)$ is then diagonal. $|P^{(l)}(t)|^2$ is the probability of the state $|n_0 + l, N - n_0 - l\rangle$ at time t and $\sum_l |P^{(l)}(t)|^2 = 1$. The linear and von Neumann entropy and the Lyapunov function can be directly obtained as follows, respectively:

$$\mathcal{S}_l(t) = 1 - \text{Tr}_1 \rho_1(t)^2 = 1 - \sum_{l=-n_0}^{N-n_0} |P^{(l)}(t)|^4, \quad (22)$$

$$\mathcal{S}_n(t) = -\text{Tr}_1 [\rho_1(t) \ln \rho_1(t)] = - \sum_{l=-n_0}^{N-n_0} |P^{(l)}(t)|^2 \ln |P^{(l)}(t)|^2, \quad (23)$$

and

$$\mathcal{V}(t) = 1 - |\langle \psi(0) | \psi(t) \rangle|^2 = 1 - |P^{(0)}(t)|^2. \quad (24)$$

The mean values of linear entropy, the von Neumann entropy, and the Lyapunov function over long time T are defined as

$$\begin{aligned} \langle \mathcal{S}_l \rangle &= \frac{1}{T} \int_0^T \mathcal{S}_l(t) dt, \\ \langle \mathcal{S}_n \rangle &= \frac{1}{T} \int_0^T \mathcal{S}_n(t) dt, \\ \langle \mathcal{V} \rangle &= \frac{1}{T} \int_0^T \mathcal{V}(t) dt. \end{aligned} \quad (25)$$

C. Coherent states

In this subsection we consider an initially disentangled product of coherent states written as

$$|\psi(0)\rangle = e^{(-|\alpha|^2 - |\beta|^2)/2} \sum_{n,m} \frac{\alpha^n}{\sqrt{n!}} \frac{\beta^m}{\sqrt{m!}} |n, m\rangle, \quad (26)$$

where α and β are the amplitudes of coherent states on subsystem 1 and subsystem 2, respectively. n and m are boson numbers (for dimer system) or vibrational quantum numbers (for molecules), with the condition $n+m=N$. The values of α and β can be any complex number, but we here let $\alpha=\beta$ be a real number. Then the initial coherent states Eq. (26) can be rewritten as the superposition of Eq. (11),

$$\begin{aligned} |\psi(0)\rangle &= e^{-\alpha^2} \sum_{N=0}^{\infty} \sum_{n_1, n_2=0}^N \frac{\alpha^N}{\sqrt{n_1! n_2!}} |n_1, n_2\rangle \\ &= \sum_{N=0}^{\infty} \sum_{n_0=0}^N \mathcal{A}_{n_0, N-n_0} |n_0, N-n_0\rangle, \end{aligned} \quad (27)$$

where $\mathcal{A}_{n_0, N-n_0} = e^{-\alpha^2} \frac{\alpha^N}{\sqrt{n_0! (N-n_0)!}}$. The sum over N is from 0 to ∞ in principle. In our numerical calculations of the entropy we truncated the sum over N at large $N = \mathcal{N}_{\max}$. We find that the $\sum_{N=0}^{\mathcal{N}_{\max}} \sum_{n_0=0}^N |\mathcal{A}|^2$ yields converged results using $\mathcal{N}_{\max} = 21$ in this work.

In a manner similar to the case of the Fock state, the time-evolved state can be obtained as follows:

$$\begin{aligned} |\psi(t)\rangle &= e^{-it\mathcal{H}} \sum_{N=0}^{\mathcal{N}_{\max}} \sum_{n_0=0}^N \mathcal{A}_{n_0, N-n_0} |n_0, N-n_0\rangle \\ &= e^{-it\mathcal{H}_0} \sum_{N=0}^{\mathcal{N}_{\max}} \sum_{n=0}^N P_{n, N-n}(t) |n, N-n\rangle, \end{aligned} \quad (28)$$

where $P_{n, N-n}(t) = \sum_{k=0}^{\infty} C_k^{n, N-n}(t)$. The recursion expression of $C_k^{n, N-n}(t)$ for the integrable dimer system is

$$\begin{aligned} C_k^{n, N-n}(t) &= -\frac{it}{k} \{ -n(N-n) C_{k-1}^{n, N-n}(t) \\ &\quad + c\sqrt{(n+1)(N-n)} C_{k-1}^{n+1, N-n-1}(t) \\ &\quad + c\sqrt{n(N-n+1)} C_{k-1}^{n-1, N-n+1}(t) \}, \end{aligned} \quad (29)$$

and for the realistic small symmetric molecule is

$$\begin{aligned} C_k^{n, N-n}(t) &= \frac{-it}{k} \left\{ \frac{\alpha}{2} \left[\left(n + \frac{1}{2} \right)^2 + \left(N - n + \frac{1}{2} \right)^2 \right] + \alpha_{12} \left(n + \frac{1}{2} \right) \left(N - n + \frac{1}{2} \right) \right\} C_{k-1}^{n, N-n}(t) + c\sqrt{(n+1)(N-n)} C_{k-1}^{n+1, N-n-1}(t) \\ &\quad + c\sqrt{n(N-n+1)} C_{k-1}^{n-1, N-n+1}(t) + \delta' \sqrt{(n+2)(N-n-1)(n+1)(N-n)} C_{k-1}^{n+2, N-n-2}(t) \\ &\quad + \delta' \sqrt{(n-1)(N-n+2)n(N-n+1)} C_{k-1}^{n-2, N-n+2}(t), \end{aligned} \quad (30)$$

where $c = \frac{1}{2}[\beta + \frac{\epsilon}{2}(N+1)]$. In Eqs. (29) and (30), $k = 0, 1, 2, \dots, \infty$, $n_0 = 0, 1, 2, \dots, N$, and the $C_{n_0, N-n_0}^{n, N-n}(t) = \mathcal{A}_{n_0, N-n_0}$ for $k=0$.

The density matrix is given by

$$\begin{aligned} \rho(t) &= |\psi(t)\rangle \langle \psi(t)| \\ &= \sum_{N, N'=0}^{\mathcal{N}_{\max}} \sum_{n=0}^N \sum_{n'=0}^{N'} P_{n, N-n}(t) \\ &\quad \times P_{n', N'-n'}^*(t) |n, N-n\rangle \langle n', N'-n'|, \end{aligned} \quad (31)$$

the corresponding reduced density matrix over subsystem 2 is given by

$$\begin{aligned} \rho_1(t) &= \text{Tr}_2 \rho(t) = \sum_{n_2} \langle n_2 | \rho(t) | n_2 \rangle \\ &= \sum_{N, n} \sum_{N', n'} P_{n, N-n}(t) \\ &\quad \times P_{n', N'-n'}^*(t) |n\rangle \langle n'| \delta_{N-n, N'-n'}. \end{aligned} \quad (32)$$

The reduced density matrix is now not diagonal. In terms of the eigenvalues $\lambda_k(t)$ of the reduced density operator, both entropies are calculated via

$$\mathcal{S}_l(t) = 1 - \sum_{k=0}^{\mathcal{N}_{\max}} [\lambda_k(t)]^2,$$

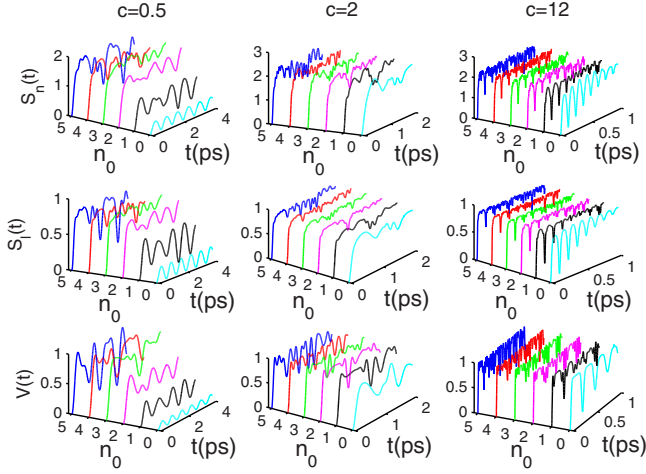


FIG. 1. (Color online) The von Neumann entropy $S_n(t)$, linear entropy $S_l(t)$, and Lyapunov function $\mathcal{V}(t)$ versus initial states $|n_0, N-n_0\rangle$ for the integrable dimer system. The total boson numbers $N=10$, $n_0=0, 1, 2, 3, 4, 5$. The coupling parameters are $c=0.5, 2$, and 12 .

$$S_n(t) = - \sum_{k=0}^{N_{\max}} \lambda_k(t) \ln \lambda_k(t). \quad (33)$$

III. RESULTS AND DISCUSSION

A. Fock states

1. Integrable dimer

We first study the properties of the quantum entanglement of the integrable dimer system. We calculate the linear and von Neumann entropy, and the Lyapunov function versus initial states $|n_0, N-n_0\rangle$ for the total boson numbers N and the different coupling parameter c . In Fig. 1, we plot $S_n(t)$, $S_l(t)$, and $\mathcal{V}(t)$ for weak coupling $c=0.5$ (the left column), medium coupling $c=2$ (the central column), and strong coupling $c=12$ (the right column) of the total boson numbers $N=10$. Because of the symmetries of Hamiltonians (2) and (5), we investigate the cases of $n_0=0, 1, \dots, \text{Fix}\{\frac{N}{2}\}$, where $\text{Fix}\{\mathcal{X}\}$ returns the integer portion of \mathcal{X} . Figure 1 shows that the entropies and the Lyapunov function for initial states $|0, N\rangle$ are periodic for weak coupling, while for the others this is not the case. Our calculations show that the oscillatory period of entropy becomes short for large N for the initial state $|0, N\rangle$. Also, the Lyapunov function is similar to entropies for the weak coupling case. The purification times of the entropy are also similar with the recurrence times of the Lyapunov function for weak coupling for the initial states $|0, N\rangle$. The entropy increases rapidly in starting time, and the entropy approaches steady state quickly with increasing coupling strength.

Figure 1 shows that the entropies and the Lyapunov function have good periodicity for $n_0=0$ for weak coupling strength $c=0.5$. However, it becomes irregular with the increasing of the n_0 in this case. The periodic behaviors are more pronounced with the increasing of the coupling

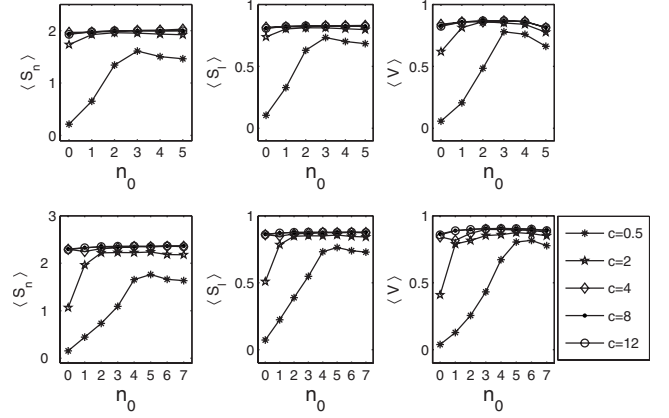


FIG. 2. The mean value $\langle S_n \rangle$, $\langle S_l \rangle$, $\langle \mathcal{V} \rangle$ versus the initial state $|n_0, N-n_0\rangle$. The $n_0=0, \dots, \frac{N}{2}$ for even N (or $\frac{N-1}{2}$ for odd N) with total boson numbers $N=10$ (top three figures), $N=15$ (bottom three figures). Five different coupling parameters are considered here, $c=0.5, 2, 4, 8$, and 12 .

strength c , and it is clearly shown that the periodic behavior is more pronounced for $c=12$ than for $c=2$ for the state $|0, N\rangle$ in the figure. It becomes “chaotic” for strong coupling.

The “accretion” of the Lyapunov function denotes that the final states are far away from the initial state. For the $N=1$ case, the explicit simple expressions for the linear entropy and the mean linear entropy are as follows:

$$S_l(t) = \frac{1}{2} \sin^2(2ct),$$

$$\langle S_l \rangle = \frac{1}{4} - \frac{1}{16cT} \sin(4cT). \quad (34)$$

These expressions clearly indicate that the linear entropy is oscillatory with the time evolution. By contrast, the mean linear entropy goes to a steady state at long time T or large cT .

The von Neumann entropy and the Lyapunov function also show similar characteristics. The mean value of the entropies and the Lyapunov function over long time T are shown in Fig. 2. It is clearly shown that the system has large entanglement for various initial states $|n_0, N-n_0\rangle$ for strong coupling ($c=4, 8, 12$). The entanglement dynamics with classical chaotic phase space for the other systems were studied by previous researchers [40–48]. Furuya *et al.* studied the entanglement process for the N -atom Jaynes-Cummings model [40], and some properties of coupled quantum kicked tops (for example, rate, the entanglement production, and the dynamics of entanglement in classically chaotic system, etc.) were also investigated [41,43,44,47]. The other interesting systems [biparticle system, AMOL (a magneto-optical lattice), etc.] were also considered [42,45,46,48]. In contrast to previous studies, we here analytically obtain the entropies and the Lyapunov function from the quantum Hamiltonian. Based on this work, we can also study the connection between quantum dynamical entanglement and classical chaos

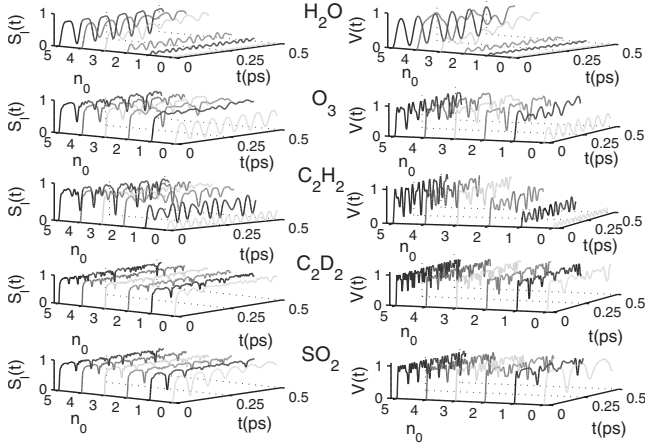


FIG. 3. The linear entropy $S(t)$ and the Lyapunov function $\mathcal{V}(t)$ as a function of evolution time t for the initial state $|n_0, N-n_0\rangle$ for molecules H_2O , O_3 , C_2H_2 , C_2D_2 , and SO_2 . The total boson numbers $N=10$, and $n_0=0, 1, 2, 3, 4, 5$. The physical parameters of the molecules are used, and they are taken from Ref. [26].

in phase space and the corresponding properties, such as the rate and the entanglement generation. The entanglement dynamics of the systems with classical chaotic phase space can be investigated via the classical limits of the quantum Hamiltonian. The classical limit of the quantum Hamiltonian Eq. (2) [and Eq. (5)] can be obtained by calculating the expectation value of quantum Hamiltonian over the coherent state [49]. However, a possible simple approach could be the use of the intensive collective boson operators introduced by Gilmore [50]. This method was used to extract the potential energy surface for small molecules [51].

For weak coupling, the average entropy increases as the initial n_0 increases, and the system is also in “chaotic sea” in this case of large n_0 . It is interesting that the average values of the entropies for the strong coupling case are almost the same. Our calculations show that such a fixed value of coupling strength is 3.8, 5.6, 7.4, 8.2, and 9.6 for $N=15, 20, 25, 30$, and 35, respectively. These values are in good agreement with the classical separatrix coupling energy [22].

2. Small molecules

In this section we calculate the linear entropy and the Lyapunov function of the small molecules H_2O , O_3 , C_2H_2 , C_2D_2 , SO_2 for the initial states $|n_0, N-n_0\rangle$. The algebraic Hamiltonian Eq. (5) developed by Kellman [26] is employed in this work. In our numerical calculations, the physical parameters of the molecules are used and they are taken from Ref. [26]. This Hamiltonian was used to study the vibrational levels, etc. [26]. In Fig. 3, we show the linear entropies (left column) and the Lyapunov function (right column) for $N=10$. We can see that the linear entropies of the molecules H_2O , O_3 , and C_2H_2 change explicitly among all the initial states, but for the molecules C_2D_2 and SO_2 the linear entropies do not vary obviously for all initial states. This could be the reason that the molecules H_2O , O_3 , and C_2H_2 have both local and normal mode character, while the molecules C_2D_2 , SO_2 have only normal mode character. The entropies for

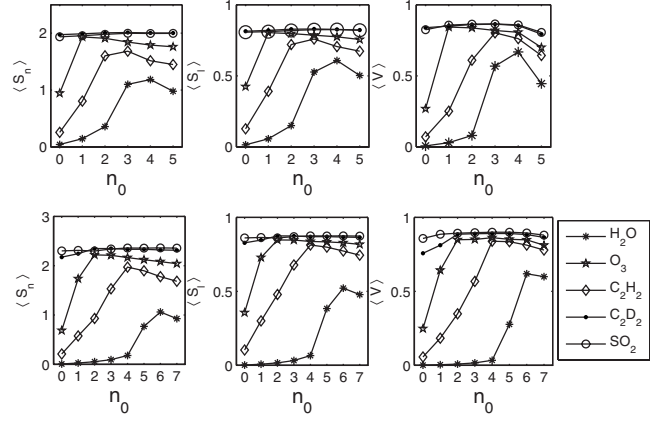


FIG. 4. The mean value of von Neumann entropy and Lyapunov function versus the initial states $|n_0, N-n_0\rangle$ with $N=10$ (top three figures) and $N=15$ (bottom three figures), $n_0=0, \dots, \frac{N}{2}$ for even N (or $\frac{N-1}{2}$ for odd N) for molecules H_2O , O_3 , C_2H_2 , C_2D_2 , and SO_2 . The physical parameters of the molecules are used, and they are taken from Ref. [26].

local initial states are quasiperiodic for molecules H_2O , O_3 , and C_2H_2 . In Fig. 3, we can also see that the entropies increase for large n_0 in the initial states $|n_0, N-n_0\rangle$ for those three molecules. Our calculations show that the oscillation frequencies become large for large N . By contrast, the entropies stay almost the same for all the initial states of the molecules C_2D_2 and SO_2 . The oscillation frequencies for those two molecules become small for large N .

In Fig. 4 we plot the mean entanglement. The turns of the mean entropies display the normal-to-local transition. The Lyapunov function also displays a similar nature to the linear entropy. The periodicity and distance between the initial states and the final states are related to the local and normal modes. This means that there is a probability to completely stay at the initial state for the local mode case and a probability to transit from the initial state to other states for the normal mode case.

3. Contributions of states to the entropy

We can understand the nature of the entropies and the contributions of states $|n_0+l, N-n_0-l\rangle$ to the entropies by analyzing the distributions of the probability $|P^{(l)}(t)|^2$ of states $|n_0+l, N-n_0-l\rangle$. In the figures showing the distributions (Figs. 5–7) of the probabilities $|P^{(l)}(t)|^2$ of states $|n_0+l, N-n_0-l\rangle$, the heights of color strip are employed to denote quantitative values of $|P^{(l)}(t)|^2$, and the different colors are used to denote the different probability $|P^{(l)}(t)|^2$. The detailed descriptions can be found in the figure captions.

Integrable dimer. Figure 5 shows the results of the probabilities $|P^{(l)}(t)|^2$ as a function of the evolution time for $N=10$ of the integrable dimer for weak (the first row, $c=0.5$), medium (the second row, $c=2$), and strong (the third row, $c=12$) coupling for the initial states $|0,10\rangle$ (the left column), $|2,8\rangle$ (the central column), and $|5,5\rangle$ (the right column). The corresponding entropies and Lyapunov function are shown in Fig. 1. From Fig. 5, for weak coupling, the main contributions are the first two states $|0,10\rangle$ and $|1,9\rangle$ for initial state

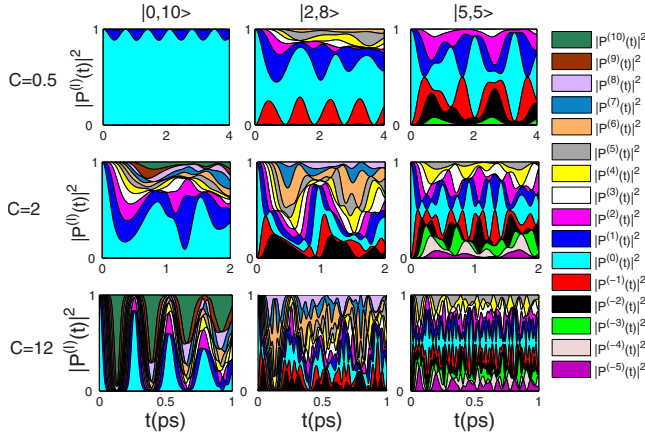


FIG. 5. (Color online) The probability $|P^{(l)}(t)|^2$ of state $|n_0+l, N-n_0-l\rangle$ as a function of the evolution time. The initial states are taken as $|n_0, N-n_0\rangle$, with total boson numbers $N=10$ and $n_0=0$ (the left column), $n_0=2$ (the central column), and $n_0=5$ (the right column). The coupling parameters are $c=0.5$ (the first row), $c=2$ (the second row), and $c=12$ (the third row). The heights of the color strips are employed to denote quantitative values of $|P^{(l)}(t)|^2$, and the different color is used to denote the different probability $|P^{(l)}(t)|^2$. The cyan strip is for $|P^{(0)}(t)|^2$.

$|0,10\rangle$. Their distributions are periodic with the evolution time, which leads to periodic entropies in this case. However, with increasing n_0 in this case (the first row in the figure), the contributions of the two states decrease and the contributions of the other states $|P^{(l)}(t)|^2$ increase; at the same time, the

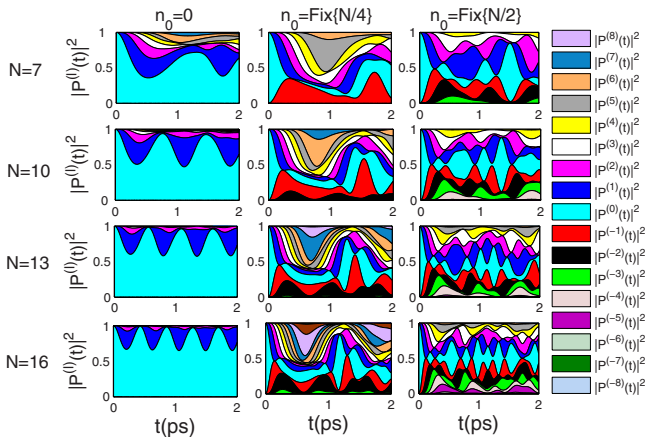


FIG. 6. (Color online) The probability $|P^{(l)}(t)|^2$ of state $|n_0+l, N-n_0-l\rangle$ as a function of the evolution time with coupling parameter $c=1.2$ for the different initial states $|n_0, N-n_0\rangle$ and N . The first row is for $N=7$ with initial states $|0, 7\rangle$ (the left column), $|1, 6\rangle$ (the central column), and $|3, 4\rangle$ (the right column). The second row is for $N=10$ with initial states $|0, 10\rangle$ (the left column), $|2, 8\rangle$ (the central column), and $|5, 5\rangle$ (the right column). The third row is for $N=13$ with initial states $|0, 13\rangle$ (the left column), $|3, 10\rangle$ (the central column), and $|6, 7\rangle$ (the right column), and the fourth row is for $N=16$ with initial states $|0, 16\rangle$ (the left column), $|4, 12\rangle$ (the central column), and $|8, 8\rangle$ (the right column). The others are the same as Fig. 5.

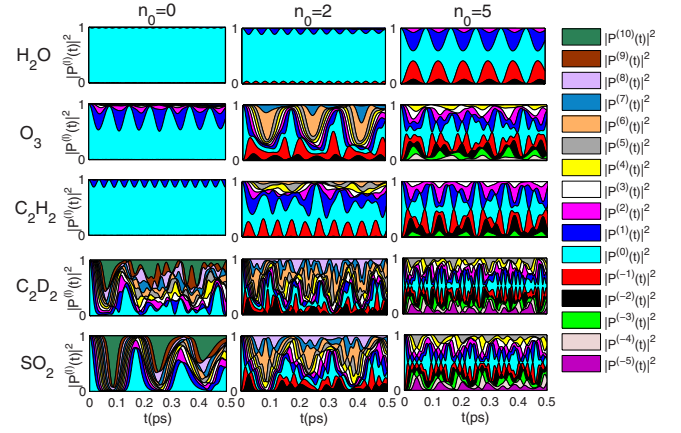


FIG. 7. (Color online) The probability $|P^{(l)}(t)|^2$ of state $|n_0+l, N-n_0-l\rangle$ for molecules H_2O , O_3 , C_2H_2 , C_2D_2 , and SO_2 with initial state $|0, 10\rangle$ (the left column), $|2, 8\rangle$ (the central column), and $|5, 5\rangle$ (the right column). The others are the same as Fig. 5.

contributions become irregular. For the symmetric initial state $|5,5\rangle$ the contributions from the states besides the initial state are also symmetric. This is shown in the right column in Fig. 5. Clearly, the main contributions are also from the states nearing initial states. For strong coupling, although the distributions of the states are regular at the initial time ($t \lesssim 0.4$ ps), this regularity becomes faint and it is finally “chaotic” for long times. The states $|0,10\rangle$ and $|10,0\rangle$ in two sides, however, have also the same contributions. For the medium coupling case, the distributions $|P^{(l)}(t)|^2$ of states are complex, as shown in Fig. 5.

To see the effect of total boson number N for the dimer system, we plot the results of the cases $N=7, 10, 13, 16$ (from first row to fourth row) with the coupling strength $c=1.2$ in Fig. 6. The initial states are chosen as $|n_0, N-n_0\rangle$ for $n_0=0$ (the left column), $n_0=\text{Fix}\{N/4\}$ (the central column), and $n_0=\text{Fix}\{N/2\}$ (the right column). For the initial state $|0, N\rangle$ ($|P^{(0)}(t)|^2$, the left column in Fig. 6), the contribution of the initial state increases with increasing N . The contributions of the first two states (here they are $|P^{(0)}(t)|^2$ and $|P^{(1)}(t)|^2$) are obviously periodic for big $N=13, 16$. However, the other initial states are not the case (the central and right columns in the figure). Especially, the contributions of “medium initial states” $|\psi(0)\rangle = |\text{Fix}\{N/4\}, N-\text{Fix}\{N/4\}\rangle$ are complex. Almost all the states, for this case, have their contributions to the entropies of the system. Similarly, for the (quasi-)symmetric initial states $|\psi(0)\rangle = |\text{Fix}\{N/2\}, N-\text{Fix}\{N/2\}\rangle$, the contributions of the states on the two sides of the initial states have the (quasi-)symmetric contributions. It is clearly shown that the states far from the initial states have less contributions to the entropies of the system.

Realistic molecules. In Fig. 7, we plot the $|P^{(l)}(t)|^2$ of the five realistic molecules with multiplet quantum numbers $N=10$ and the initial states $|0,10\rangle$ (the left column), $|2,8\rangle$ (the central column), and $|5,5\rangle$ (the right column). It is clearly shown that the $|P^{(l)}(t)|^2$ of molecules H_2O , O_3 , C_2H_2 have

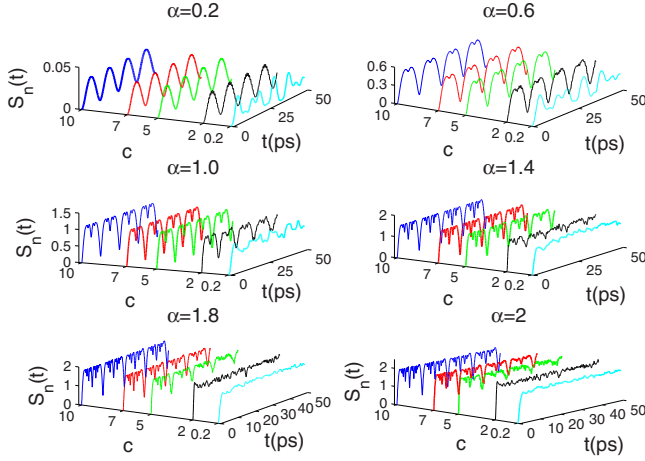


FIG. 8. (Color online) The von Neumann entropy $S_n(t)$ as a function of the evolution time. The different coupling parameters c and coherent amplitude α are chosen for the integrable dimer system. The detail values are marked in the figure.

periodicity (see Fig. 3). Again, the probabilities $|P^{(l)}(t)|^2$ of states $|n_0-l, N-n_0+l\rangle$ have the symmetric distributions for the symmetric initial states (the right column in the figure). This demonstrates that the vibrations of the three molecules are in the local mode. By contrast, the molecules C_2D_2 , SO_2 have no periodicity, and they are in the “chaotic sea.” Physically, the two molecules exhibit strong entanglement, and their vibrations are in the normal modes.

The contributions of the states in the H_2O molecule are periodic. The entropies of the H_2O molecule are (quasi-)periodic for all initial states with $N=10$, and the entropies increase with increasing n_0 (from the left to the right column in the figure). This leads to the periodicity of entanglement and the disentanglement of the H_2O molecule. The $|P^{(l)}(t)|^2$ of molecules O_3 and C_2H_2 have no periodicities for $n_0=2$ and 5. It is shown, in Fig. 3, that their entropies vary irregularly for the initial states $|2,8\rangle$ and $|5,5\rangle$. However, the molecules C_2D_2 and SO_2 are different from the other three molecules. Even the distributions of $|P^{(l)}(t)|^2$ seem regular at the starting time for $|0,10\rangle$; the distributions are becoming “chaotic” with time evolution, especially for the molecule C_2D_2 .

B. Coherent states

Figures 8 and 9 show the von Neumann entropy with initially disentangled coherent states. In Fig. 8, we plot the von Neumann entropy for different coupling parameter c and coherent amplitude α for the integrable dimer. The system has purification time or near disentangled states for small coherent amplitude $\alpha=0.2$, and 0.6 from weak coupling to strong coupling. It is interesting that the von Neumann entropy of the disentangled dimer has good periodicity for the strong coupling but for the weak coupling $c=0.2$ for the small coherent amplitude α . However, for weak coupling ($c=0.2$), this periodicity disappears completely with increasing coherent amplitude α . The amplitude of the entropies increase with the coherent amplitude α for all the coupling cases.

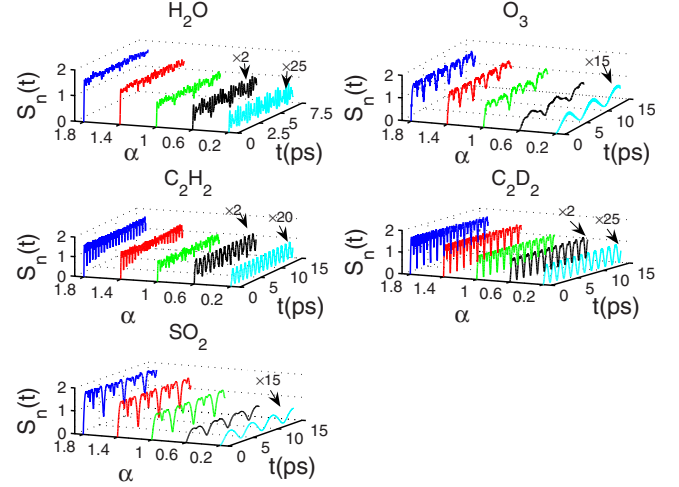


FIG. 9. (Color online) The von Neumann entropy $S_n(t)$ as a function of the evolution time. The different coherent amplitude α for molecules H_2O , O_3 , C_2H_2 , C_2D_2 , and SO_2 are plotted, the values of α are marked in the figure. To see clearly, some of the entropies were amplified and they are marked in the figure.

The von Neumann entropies of the molecules H_2O , O_3 , C_2H_2 , C_2D_2 , SO_2 are given in Fig. 9. The von Neumann entropies are (quasi-)periodic for small coherent amplitude except for the H_2O molecule. It is interesting that the von Neumann entropy of the H_2O molecule has “classical”-like beat phenomena. This could show the properties of the weak coupling strength of the H_2O molecule, physically. It is also shown that, for the small coherent amplitude $\alpha=0.2$, the entropies of the other four molecules (O_3 , C_2H_2 , C_2D_2 , and SO_2) have a good periodicity. With the increasing of the coherent amplitude α , the more frequencies of the entropy for coherent states are presented.

IV. CONCLUSION

We studied the dynamical entanglement of the integrable dimer and the realistic small symmetric molecules in the initial Fock states and the coherent states. Our studies show that the periodicity of entanglement not only depends on the coupling strength of the two subsystems but also the initial states. For the integrable dimer system, in the case of weak coupling and initial state $|0, N\rangle$, the purification time is the recurrence time. For the molecules H_2O , O_3 , C_2H_2 , C_2D_2 , SO_2 , it is found that the periodicity of the entanglement with local-mode initial states is better than with normal-mode initial states. The explicit changes of the entropy and the sharp peak of their mean values display the normal-to-local transition of the molecular vibrations. For the “biased initial state” $|\psi(0)\rangle=|0, N\rangle$, only a few states “close to” the initial states have obvious contributions to the entropies. However, with the increasing of the boson number n_0 of initial state $|n_0, N-n_0\rangle$ in “subsystem 1,” the more states will have contributions to entropy and the contributing weights of the states close to the initial states become less. When the initial state is (quasi-)symmetric state $|\psi(0)\rangle=|\text{Fix}\{N/2\}, N-\text{Fix}\{N/2\}\rangle$, the contributions to the entropy from the two sides of the

initial state $|\psi(0)\rangle$ are also (quasi-)symmetric. For the initial coherent states, the von Neumann entropy is periodic for small coherent amplitude even for the strong coupling of the dimer and molecular system.

More fundamental extensions are also possible. The dynamical entanglement of realistic small molecules in an external laser field could be (analytically) studied via the algebraic approach in the interaction picture.

ACKNOWLEDGMENTS

We much appreciate the referee's suggesting Refs. [40–48] and careful comments on the manuscript. This work was supported by the National Science Foundation of China (Grants No. 10674083, No. 10874102, and No. 10474058). Partial financial support from the Science Foundation of Shandong Province, China and the project sponsored by SRF for ROCS, SEM.

-
- [1] S. Loyd, *Science* **261**, 1589 (1993).
 [2] S. J. Gu, S. S. Deng, Y. Q. Li, and H. Q. Lin, *Phys. Rev. Lett.* **93**, 086402 (2004).
 [3] C. H. Bennett and S. J. Wiesner, *Phys. Rev. Lett.* **69**, 2881 (1992).
 [4] S. Hill and W. K. Wootters, *Phys. Rev. Lett.* **78**, 5022 (1997).
 [5] C. H. Bennett, G. Brassard, C. Crepeau, R. Jozsa, A. Peres, and W. K. Wootters, *Phys. Rev. Lett.* **70**, 1895 (1993).
 [6] R. Cleve, D. Gottesman, and H. Lo, *Phys. Rev. Lett.* **83**, 648 (1999).
 [7] X. W. Hou, M. F. Wan, and Z. Q. Ma, *Chem. Phys. Lett.* **426**, 469 (2006); X. W. Hou, J. H. Chen, and B. Hu, *Phys. Rev. A* **71**, 034302 (2005).
 [8] S. D. Du and C. D. Gong, *Phys. Rev. A* **50**, 779 (1994).
 [9] O. Osenda and P. Serra, *Phys. Rev. A* **75**, 042331 (2007).
 [10] V. S. Malinovsky and I. R. Sola, *Phys. Rev. Lett.* **96**, 050502 (2006).
 [11] C. H. Bennett, D. P. DiVincenzo, J. A. Smolin, and W. K. Wootters, *Phys. Rev. A* **54**, 3824 (1996).
 [12] C. H. Bennett, G. Brassard, S. Popescu, B. Schumacher, J. A. Smolin, and W. K. Wootters, *Phys. Rev. Lett.* **76**, 722 (1996).
 [13] V. Vedral, M. B. Plenio, M. A. Rippin, and P. L. Knight, *Phys. Rev. Lett.* **78**, 2275 (1997).
 [14] J. Gong and P. Brumer, *Phys. Rev. A* **68**, 022101 (2003).
 [15] S. Schneider and G. J. Milburn, *Phys. Rev. A* **65**, 042107 (2002).
 [16] W. H. Zurek, *Rev. Mod. Phys.* **75**, 715 (2003).
 [17] H. K. Park and S. W. Kim, *Phys. Rev. A* **67**, 060102(R) (2003).
 [18] M. Hiller, T. Kottos, and A. Ossipov, *Phys. Rev. A* **73**, 063625 (2006).
 [19] R. Franzosi and V. Penna, *Phys. Rev. A* **63**, 043609 (2001); R. Franzosi, V. Penna, and R. Zecchina, *Int. J. Mod. Phys. B* **14**, 943 (2000).
 [20] G. Kalosakas, A. R. Bishop, and V. M. Kenkre, *Phys. Rev. A* **68**, 023602 (2003); G. Kalosakas and A. R. Bishop, *ibid.* **65**, 043616 (2002).
 [21] M. Albiez, R. Gati, J. Fölling, S. Hunsmann, M. Cristiani, and M. K. Oberthaler, *Phys. Rev. Lett.* **95**, 010402 (2005).
 [22] S. Aubry, S. Flach, K. Kladko, and E. Olbrich, *Phys. Rev. Lett.* **76**, 1607 (1996).
 [23] C. M. Tesch and R. de Vivie-Riedle, *Phys. Rev. Lett.* **89**, 157901 (2002).
 [24] D. Babik, *J. Chem. Phys.* **121**, 7577 (2004).
 [25] T. Cheg and A. Brown, *J. Chem. Phys.* **124**, 034111 (2006).
 [26] M. E. Kellman, *J. Chem. Phys.* **83**, 3843 (1985).
 [27] P. J. Wang and G. Z. Wu, *Phys. Rev. A* **66**, 022116 (2002).
 [28] S. Keshavamurthy, *J. Chem. Phys.* **122**, 114109 (2005).
 [29] J. Zúñiga, J. Antonio *et al.*, *J. Chem. Phys.* **126**, 244305 (2007).
 [30] T. Sako, K. Yamanouchi, and F. Iachello, *J. Chem. Phys.* **114**, 9441 (2001).
 [31] L. Sanz, R. M. Angelo, and K. Furuya, *J. Phys. A* **36**, 9739 (2003).
 [32] Y. X. Liu, S. K. Özdemir, A. Miranowicz *et al.*, *J. Phys. A* **37**, 4423 (2004).
 [33] M. E. Kellman and V. Tyng, *Phys. Rev. A* **66**, 013602 (2002).
 [34] C. H. Bennett, H. J. Bernstein, S. Popescu, and B. Schumacher, *Phys. Rev. A* **53**, 2046 (1996).
 [35] A. Isar, *Fortschr. Phys.* **47**, 855 (1999).
 [36] M. Mirrahimi, G. Turinici, and P. Rouchon, *J. Phys. Chem. A* **109**, 2631 (2005).
 [37] K. Beauchard, J. M. Coron, M. Mirrahimi, and P. Rouchon, *Syst. Control Lett.* **56**, 388 (2007).
 [38] M. Mirrahimi and R. V. Handel, *SIAM J. Control Optim.* **46**, 445 (2007); M. Mirrahimi, P. Rouchon, and G. Turinici, *Automatica* **41**, 1987 (2005).
 [39] S. Ceng, *Introduction to Quantum Mechanical System Control* (Scientific Press, Beijing, 2006).
 [40] K. Furuya, M. C. Nemes, and G. Q. Pellegrino, *Phys. Rev. Lett.* **80**, 5524 (1998).
 [41] P. A. Miller and S. Sarkar, *Phys. Rev. E* **60**, 1542 (1999).
 [42] S. Bettelli and D. L. Shepelyansky, *Phys. Rev. A* **67**, 054303 (2003).
 [43] A. Lakshminarayan, *Phys. Rev. E* **64**, 036207 (2001).
 [44] H. Fujisaki, T. Miyadera, and A. Tanaka, *Phys. Rev. E* **67**, 066201 (2003).
 [45] A. J. Scott and C. M. Caves, *J. Phys. A* **36**, 9553 (2003).
 [46] Ph. Jacquod, *Phys. Rev. Lett.* **92**, 150403 (2004).
 [47] X. Wang, S. Ghose, B. C. Sanders, and B. Hu, *Phys. Rev. E* **70**, 016217 (2004).
 [48] S. Ghose and B. C. Sanders, *Phys. Rev. A* **70**, 062315 (2004).
 [49] W. M. Zhang, D. H. Feng, and R. Gilmore, *Rev. Mod. Phys.* **62**, 867 (1990).
 [50] R. Gilmore, *Catastrophe Theory for Scientists and Engineers* (Wiley, New York, 1981).
 [51] S. Ding and Y. Zheng, *J. Chem. Phys.* **111**, 4466 (1999); Y. Zheng and S. Ding, *Phys. Rev. A* **64**, 032720 (2001).